Article ID: 1003- 6326(2000)02- 0131- 08

Correlation of seawater corrosion and processing of Cu-Ni alloy tubes①

ZHU Xiao-long(朱小龙)
General Research Institute for Nonferrous Metals, Beijing 100088, P. R. China

Abstract: The investigations on the effect of the initial surface and microstructure on the seawater corrosion of Cu-Ni alloy tubes were carried out by processing, electrochemical methods and natural seawater exposure as well as SEM. Deformation had more impact on the final microstructure of the tubes than the annealing time did, and at the deformation of 32% and annealing temperature 550~ 600 ℃ for 1 h the tubes was completely recrystallized microstructure. As increasing the volume fraction of recrystallization, the homogeneity of microstructure and the corrosion resistance increased. The residual carbon film produced on the inner surface of the tubes during the processing, had higher corrosion potential than the alloy substrate and good electronic conductivity, so accelerating the dissolution of the substrate in seawater, and the non-protective and loose corrosion product film formed. Immersed in natural seawater, the tubes of incomplete recrystallization, consisting of deformed and recrystallized grains, displayed intergranular corrosion, which resulted from corrosion micro-cells built between deformed and recrystallized grains and the preferable transportation of electrons on the boundaries of both the grains. In contrast, the recrystallized alloy tubes formed the uniform and compact corrosion product film under which no corrosion was found.

Key words: Cu-Ni alloy tubes; processing; recrystallization; residual carbon film; seawater corrosion
Document code: A

1 INTRODUCTION

Cu-Ni alloys have been primarily used as tubes for condensers and heat exchangers since they came into practical use in 1950's. As the alloys have excellent corrosion and biofouling resistance to seawater, their applications in marine engineering have been rapidly developed. However, some early failure and serious corrosion occasionally occur to Cu-Ni alloys during their service. Extensive researches have been carried out mostly on chemical compositions, initial surface films and environmental factors during their service[1~3]. Some measures, e. g. the addition of alloy elements with certain content, surface pretreatment and pre-formation of the film in clean seawater, have ever been taken to prolong the service life of the alloys to some degree. But the measures cannot completely prevent the early failure of the alloys.

By different heat treatment to obtain the microstructures with homogeneous solid solution, continuous precipitates or discontinuous precipitates, Drolenga et al[4] notified the influence of microstructure on the corrosion behavior of Cu-Ni alloys. They demonstrated that the corrosion resistance of the alloy with discontinuous precipitate was distinctly low in seawater. Since their processing parameters for the alloys were far from those in industrial production, no discontinuous precipitate could be observed even for commercial Cu-Ni alloys annealed at 450 ℃ for 4 h[5]. Some research verified that particles rich in Ni-Fe formed during slow cooling for 90Cu-10Ni and 70Cu-30Ni alloys[6]. Thus, it still needs to explore how to eliminate and inhibit the occurrence of the discontinuous precipitates and correlate the processing and corrosion of Cu-Ni alloys.

As shown in the author's previous work, the deformation and heat treatment can change the microstructure of Cu-Ni alloys and so influence their corrosion resistance[7]. This paper is to investigate the relationship of processing, microstructure and corrosion, applying deformation and heat treatment to commercial Cu-Ni alloy tubes and further comparing their corrosion data and behaviors in seawater.

2 EXPERIMENTAL

2.1 Materials

Specimens were cut from commercial 70Cu-30Ni alloy tubes, and their chemical compositions and processing are listed in Table 1.

The microstructure of the specimen was observed on an optical microscope (Neophot 2, Denmark). The volume fraction of recrystallization was ascertained by line analysis, i. e. four intersection lines in the metallograph were chosen to form angle 45° by each other. The ratio of the recrystallization per unit length in the lines stands for the volume fraction of recrystallization.

① **Foundation item:** Project 59290900 supported by the National Natural Science Foundation of China
Received date: Aug. 5, 1999; **accepted date:** Jan. 10, 2000

Table 1 Chemical compositions and processing of 70Cu-30Ni alloy tubes

Specimen	Chemical composition(mass fraction, %)	Processing
A	Ni29.58, Fe0.89, Mn0.89, Si0.19, Co< 0.01, Pb0.0001, Cu Bal.	Melting → Semi-casting → Pressing(1020 ℃) → Drawing → Annealing → … → Drawing(11%) → Annealing(550~ 600 ℃) 1 h
B	Cu70.08, Ni28.72, Fe0.54, Mn0.66	Melting → Semi-casting → Pressing(1020 ℃) → Drawing → Annealing → … → Drawing(21%) → Annealing(550~ 600 ℃) 0.5 h
C	Cu70.08, Ni28.72, Fe0.54, Mn0.66	Melting → Semi-casting → Pressing(1020 ℃) → Drawing → Annealing → … → Drawing(21%) → Annealing(550~ 600 ℃) 1 h
D	Cu70.08, Ni28.72, Fe0.54, Mn0.66	Melting → Semi-casting → Pressing(1020 ℃) → Drawing → Annealing → … → Drawing(32%) → Annealing(650 ℃) 1 h
E	Ni29.51, Fe0.39, Mn0.78, Si0.07, Pb< 0.02, P< 0.03, Cu Bal.	Melting → Semi-casting → Pressing(1040 ℃) → Drawing → Annealing → … → Drawing(24%) → Annealing(550~ 600 ℃) 1 h
F	Ni30.08, Fe0.30, Mn0.60, Si0.09, Pb< 0.02, P< 0.03, Cu Bal.	Melting → Semi-casting → Pressing(1040 ℃) → Drawing → Annealing → … → Drawing(28%) → Annealing(550~ 600 ℃) 1 h
G	Ni29.39, Fe0.43, Mn0.85, Si0.09, P< 0.03, Pb< 0.02, Cu Bal.	Melting → Semi-casting → Pressing(1040 ℃) → Drawing → Annealing → … → Drawing(32%) → Annealing(550~ 600 ℃) 1 h
H	Ni30.79, Fe0.85, Mn0.87, P0.0001, Cu Bal.	Melting → Semi-casting → Pressing(1040 ℃) → Drawing → Annealing → … → Drawing(35%) → Annealing(550~ 600 ℃) 1 h

2.2 Electrochemical analysis

Specimens were polished to sandpaper No. 800 and rinsed by water, and then degreased by acetone and dried by wind dryer. Table 2 lists the chemical composition of corrosion medium, i.e. synthetic seawater, and S^{2-} ions were introduced to synthetic seawater (2×10^{-6} g/L) by adding Na_2S. The electrochemical experiments from cathodic to anodic polarization were carried out on Corrosion Measurement System Model 351 (Princeton Corp. US) and scanning velocity was 10 mV/min. Cyclic polarization curves were obtained from φ_c(corrosion potential) − 100 mV ~ φ_c+ 150 mV and then reversed scanned to φ_c− 50 mV (scanning velocity was 10 mV/min).

Table 2 Chemical composition of artificial seawater (from Lyma and Fleming)[8]

Salt	Mass/g	Salt	Mass/g
NaCl	23.476	$NaHCO_3$	0.192
$MgCl_2$	4.981	KBr	0.095
Na_2SO_4	3.917	H_3BO_3	0.025
$CaCl_2$	1.102	$SrCl_2$	0.024
KCl	0.664	NaF	0.003

Adding water to 1000 g in total

2.3 Natural seawater exposure and corrosion product analysis

Natural seawater immersion was in Qingdao Seawater Corrosion Station (36°03′ north latitude, and 120°25′ east longitude) and the main environmental factors are listed as Table 3. Exposure was in full immersion (1.5~ 5.0 m below seawater). Before immersion in seawater, specimens (d25 mm × 200 mm × 1 mm) were degreased by acetone and other organic dissolvent and dried for 24 h, and weighed on the balance with high precision to 1 mg twice. After immersion, specimens were put into 10% H_2SO_4 solution to remove the corrosion product, degreased and dried for 24 h, and then weighed on the balance with the same precision as before. The corrosion rate can be calculated as follow formula:

$$\text{Average corrosion rate} = KW/(At\rho)\ (\text{mm/a})$$

where K —Constant, 3.65×10^3; W —Loss of mass, $W = m_{\text{original}} - m_{\text{corrosion}}$; A —Area of specimen, cm^2; t —Exposure time, day; ρ—Density of specimen.

Immersed in natural seawater for different periods of time, specimens formed corrosion product films on their surface and the films were analyzed by SEM and EDX.

3 RESULTS AND ANALYSIS

3.1 Microstructure

Specimen A with incomplete recrystallization was composed of deformed and recrystallized grains (Fig. 1). Both of specimen B and C displayed incomplete recrystallization. However, the grain size of specimen C was a little bigger than that of specimen B though the annealing time of specimen C is twice that of specimen B. As increasing deformation to 32%, specimen D is completely recrystallized (Fig. 1(b)), and so deformation has more effect on the microstructure than the annealing time. Specimen E and F were of incomplete recrystallization, whereas specimen G and H of recrystallization (Fig. 1(c)). Specimen G indicated finer grains than specimen D or H, and the grain size of specimen H was almost the same but that specimen G with fine grains demonstrated very different grain size.

Table 3 Main environmental factors of Qingdao Seawater Corrosion Station

Salt /(g·L^{-1})	Dissolved oxygen/(mL·L^{-1})	pH	Temperature/ ℃			Flowing velocity/(m·s^{-1})	Tide half-day average tide difference/ m
			High	Low	Average		
32.23	5.57	8.16	27	1.1	13.6	0.1	2.7

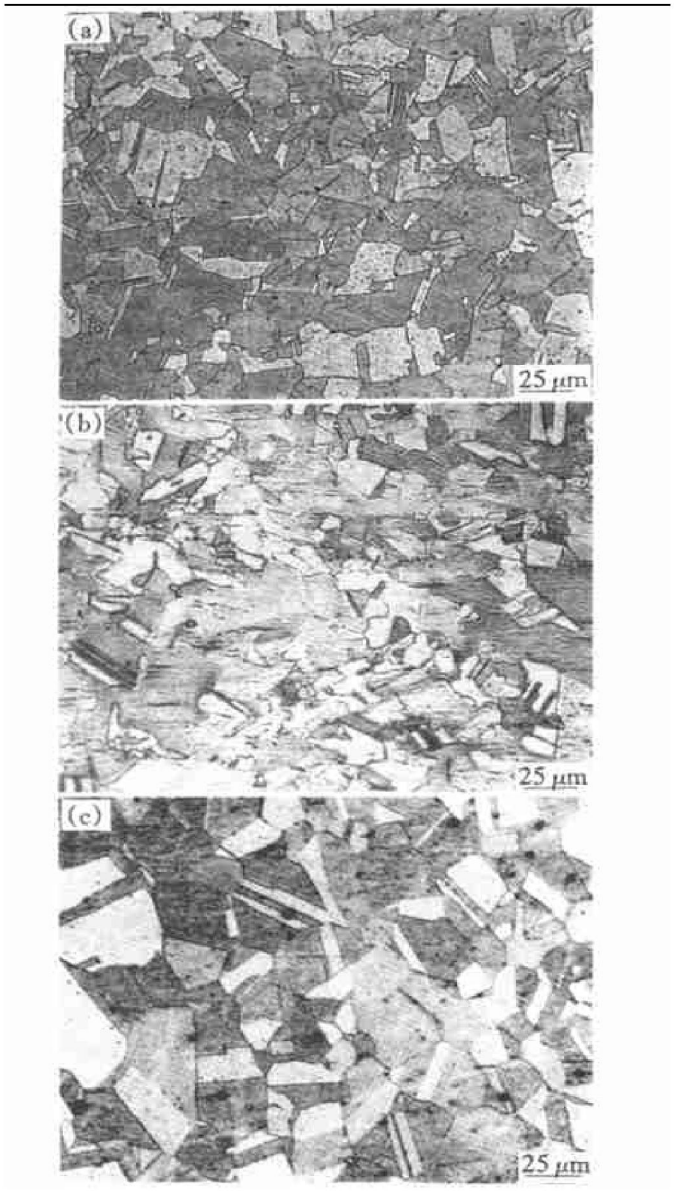

Fig. 1 Microstructures of Cu-Ni alloy tubes
(a) —Specimen A; (b) —Specimen D; (c) —Specimen H

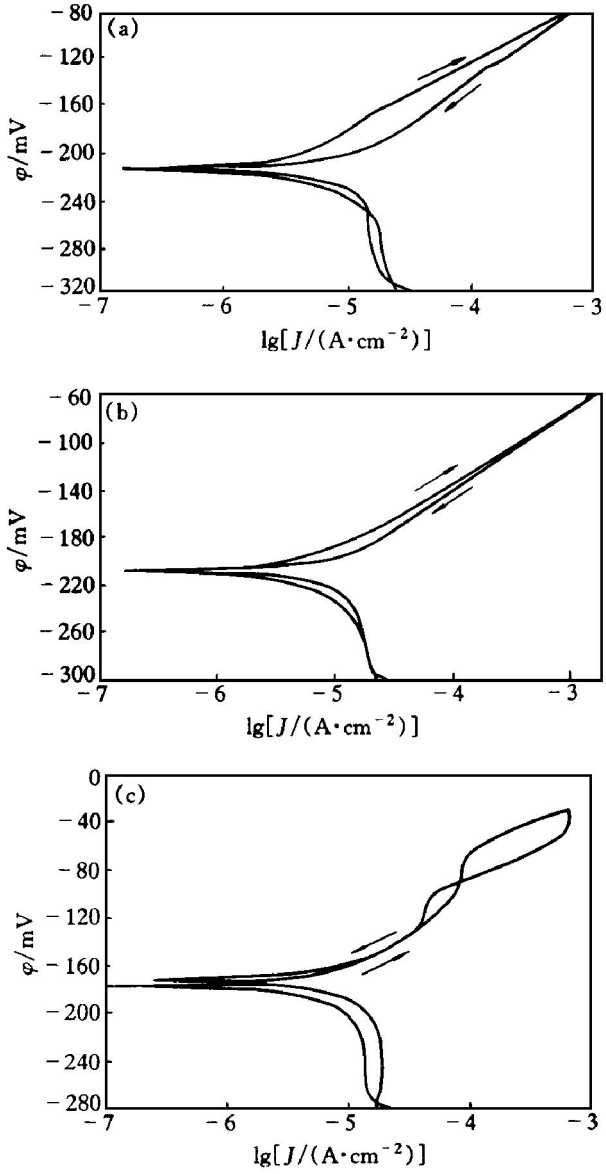

Fig. 2 Cyclic polarization curves of Cu-Ni alloy tubes in synthetic seawater containing 2×10^{-6} g/L S^{2-}
(a) —Specimen B; (b) —Specimen C; (c) —Specimen D

3.2 Electrochemical investigations in synthetic seawater

The cyclic polarization curves for specimen B, C and D in synthetic seawater with the addition of 2×10^{-6} g/L S^{2-} ions are shown in Fig. 2. Supposing the initial potential and the potential (reversal scanning to where current is zero ($I=0$)) were φ_c and φ_o, respectively, specimen B and C indicated low pitting resistance since the oxide films formed by anodic polarization were poorly protective for $\varphi_o<\varphi_c$ (specimen B) or $\varphi_o=\varphi_c$ (specimen C). The current density of specimen D was high at first and rapidly decreased when the potential reverse scanned, so the specimen displayed more resistant to pitting for $\varphi_o>\varphi_c$, i.e. the oxide film by anodic polarization was more stable than that without the film. All the cathodic parts of the specimens reached the oxygen diffusion limit current.

Both the inner and the outer surface of specimen E, F and G immersed in synthetic seawater for 20 d were tested by electrochemical polarization (Fig. 3 and 4). As to the cathodic polarization of the inner surfaces (Fig. 3(a)), specimen F had both the lowest corrosion potential and current density, which was not up to oxygen diffusion limit current, and specimen E was similar to specimen F either in the cathodic or in the anodic polarization (Fig. 3(b)). With the

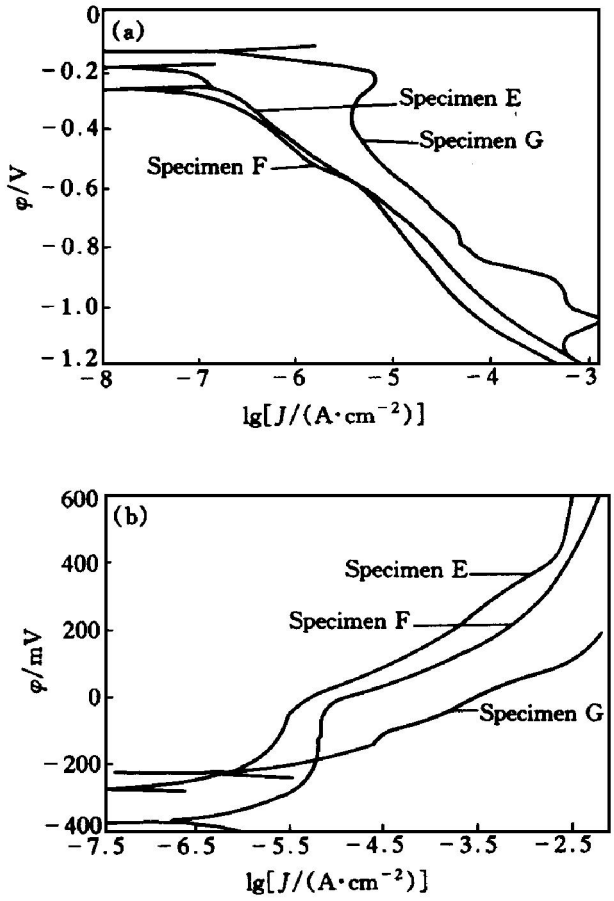

Fig. 3 Polarization curves of inner surface of Cu-Ni alloy tubes immersed in synthetic seawater for 20 d
(a) —Cathodic; (b) —Anodic

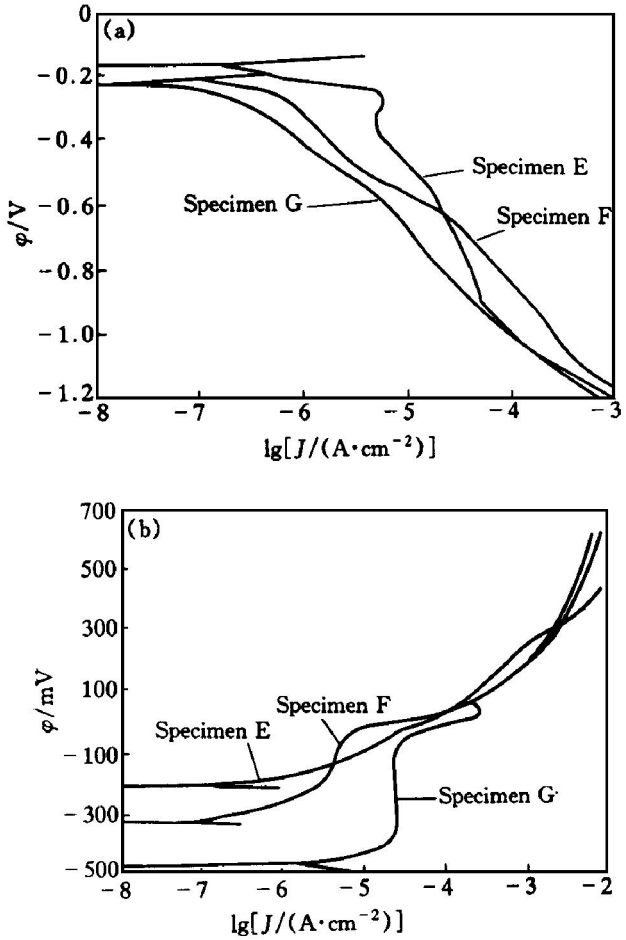

Fig. 4 Polarization curves of outer surface of Cu-Ni alloy tubes immersed in synthetic seawater for 20 d
(a) —Cathodic; (b) —Anodic

highest corrosion potential, specimen G showed the rapid increase of cathodic or anodic current density, which can be ascribed to the residual carbonaceous film formed on the surface during processing. The superior electronic and ionic conductivity of the residual carbonaceous film has nearly no barrier for the electronic transportation of the cathodic polarization or for anodic dissolution and besides the potential of the film is higher than the alloy substrate in seawater. Thus, the alloy is accelerated to dissolve as an anode of corrosion cells built between the alloy and the carbonaceous film and so the initial corrosion product film is porous and loose[9, 10]. With the increase of immersion time in synthetic seawater, the corrosion potential of Cu-Ni alloys shifted to negative for the reason of the Ni enrichment in the surface corrosion product film[11, 12]. As the cathodic polarization curves can reflect the electronic conductivity of the corrosion product film formed on the surface, the corrosion product films of specimen E and F were more resistant to the electronic migration than that of specimen G during corrosion since the former showed a lower electronic conductivity. Both specimen E and F had passive zones and their corrosion potential needed longer time to return to the original value than that of specimen G after cathodic polarization. Therefore, it verifies that the corrosion product films for specimen E and F are low in electronic conductivity, i. e. high resistance of cathodic process and more resistant to the dissolution of the anodic process. Specimen E displayed lower current density and a narrower passive zone than specimen F for anodic polarization. No passive zone was observed in the anodic polarization curve and the current density increased rapidly for specimen G. Hence, the initial corrosion product film of specimen G provided low resistance to the dissolution of the alloy.

From the polarization curves of the outer surface (Fig. 4), specimen G kept the lowest current density of the cathodic polarization and had a wide passive zone in the anodic polarization curve. Consequently, the immersion film formed on the outer surface was low in ionic and electronic conductivity and so was protective, and this was related to no residual carbonaceous film on the outer surface. The current density of specimen E was high and increased rapidly either in cathodic or anodic polarization, and there was a peak in the cathodic polarization curve. Specimen F kept between specimen E and G in the current density of cathodic polarization and had a passive zone, which

was not so wide as that of specimen G in the anodic polarization curve. The polarization curves display the corrosion resistance of the alloy tubes themselves since there is no residual carbonaceous film formed on their outer surface during processing. Both specimen F and G can form protective corrosion product films, while specimen E only forms the dissolvable corrosion product film on the surface in seawater.

As to current peaks between the potential – 250 and – 350 mV for the inner surface of specimen G and the outer surface of specimen E, Bjourndahl and Nobe[13] speculated that the corresponding initial corrosion product was CuCl on the thermodynamics theory. Moreau[14] confirmed that the surface on the electrode was CuCl by X-ray. Actually the distinct increase of the current density demonstrates that some species are involved in the cathodic process and so the peak in the cathodic polarization curve results from the reduction of CuCl. The rapid decrease of the current density after the peak is called as "cathodic passivation", which is from the following reaction according to Dhar et al[15].

$$CuCl_2^- + e = Cu + 2Cl^-$$

The other cathodic peak occurred at c. a. – 900 mV on the inner surface of specimen G and the position of this peak should correspond to the potential of the reduction of Cu_2O[16].

In the anodic process, the passive zone, i. e. the formation of the film Cu_2O, shows the stability of the surface film by means of its width. The formation of the passive film enhances the resistance of ionic and electronic migration, but the alloy tube without a passive zone is in the active state and forms dissolvable compounds when exposed to seawater.

The polarization curves of the inner surface of specimen A and H in synthetic seawater are shown in Fig. 5. The current density of the cathodic polarization for specimen H was lower than that for specimen A and both had a passive zone in the anodic polarization curves, but specimen H demonstrated lower passive current density than specimen A. From the polarization curves of the outer surface (Fig. 6), the anodic current density of specimen H was lower than that of specimen A. Also, specimen H had a passive zone in the anodic polarization curve, whereas specimen A kept active according to the anodic polarization curve. The results of the inner surface should be influenced primarily by the initial surface and the effect of the initial surface would disappear after corrosion for a period of time.

3.3 Corrosion in natural seawater

After being immersed in natural seawater for 4 months (Fig. 7), the loose corrosion product film was formed on the inner surface of specimen B and under the film intergranular corrosion occurred. In regard to specimen C, the outer layers were loose and porous

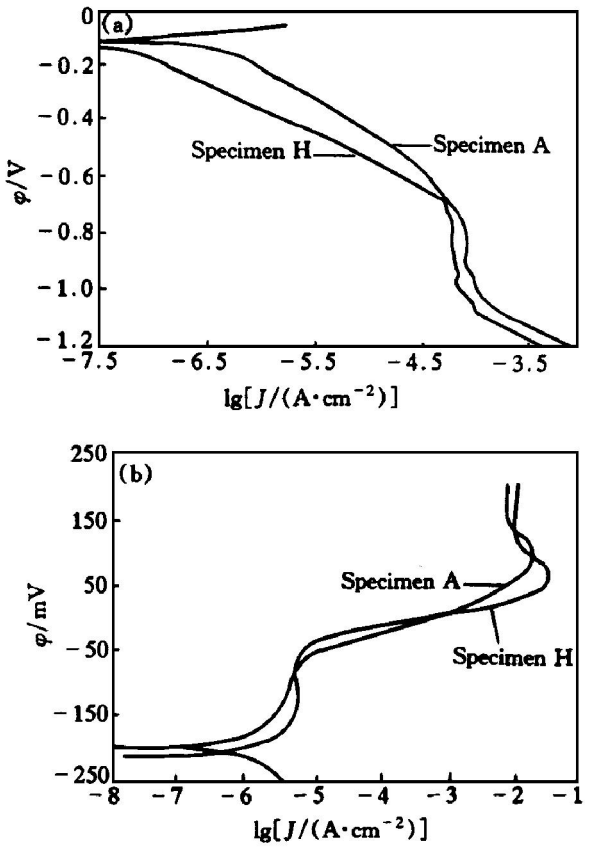

Fig. 5 Polarization curves of inner surface of Cu-Ni alloy tubes in synthetic seawater
(a) —Cathodic; (b) —Anodic

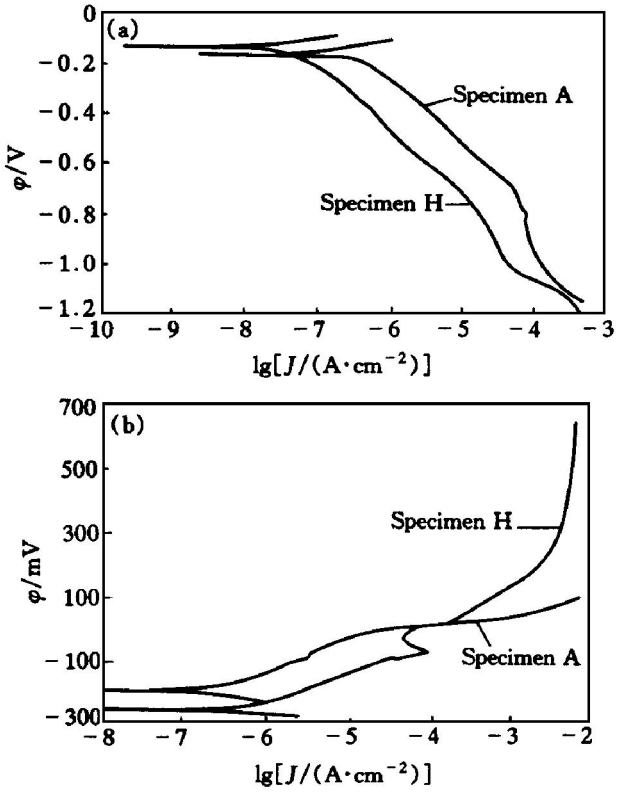

Fig. 6 Polarization curves of outer surface of Cu-Ni alloy tubes in synthetic seawater
(a) —Cathodic; (b) —Anodic

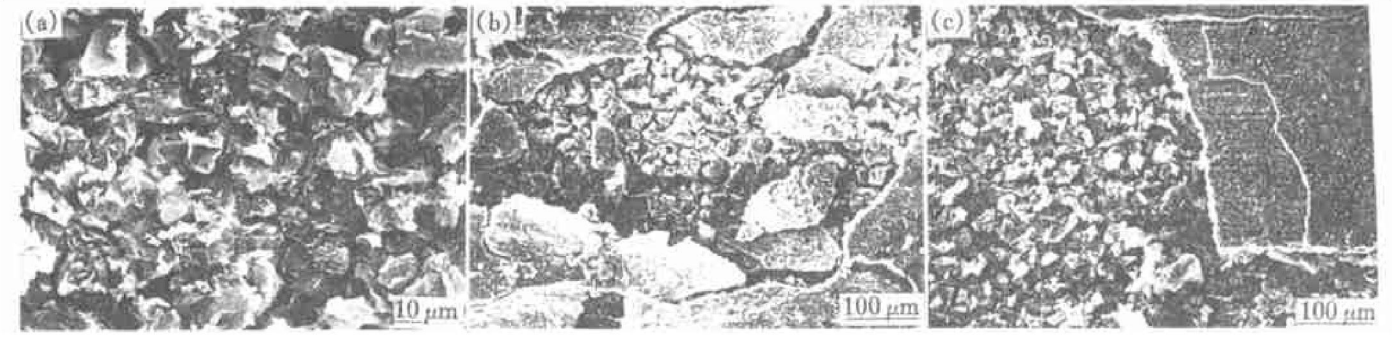

Fig. 7 Corrosion morphologies of Cu-Ni alloy tubes immersed in natural seawater for 4 months
(a) —Specimen B; (b) —Specimen C; (c) —Specimen D

and the next layer scaled off. The next layer of specimen D was rich in Ni, smooth and compact though the outer layer was also loose. Fig. 8 displays the results of specimen A and H immersed in severely polluted seawater and specimen E, F and G immersed in clean seawater for 1, 2 and 4 a, respectively. The corrosion rates of specimen E and F seemed to be not high, but their corrosion was serious from SEM observation and both had intergranular corrosion even if they were exposed to clean seawater. Specimen G showed low corrosion rate and the uniform and compact surface film.

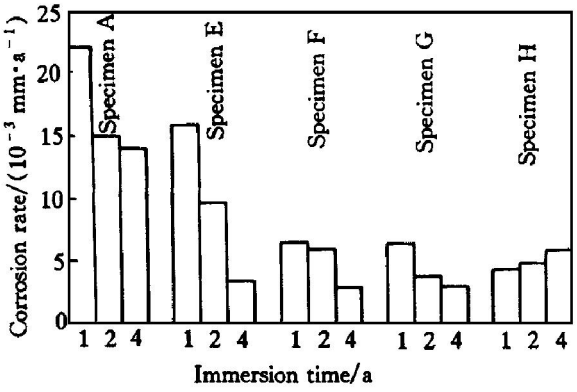

Fig. 8 Corrosion data of Cu-Ni alloy tubes immersed in natural seawater

After immersion in seawater for 48 months, specimen H showed the least corrosion and the thin, uniform and compact corrosion product film was formed on its surface (Fig. 9(a)). By EDX analysis, the film was rich in Ni and low in seawater species and no corrosion was found under the film. In contrast, the corrosion rate of specimen A was high and perforated after seawater exposure for 48 months. Also, the corrosion product film was loose and corrosion proceeded along certain boundaries between grains, particularly even one whole grain or several grains fell off for intergranular corrosion (Fig. 9(b)).

After 12 month immersion in natural seawater, the corrosion characteristics of specimen E, F and G were shown in Fig. 10. Some cracks existed on the outer layer of specimen E and the size on grains was very different where intergranular corrosion occurred (Fig. 10(a)). For specimen F, the outer layer also had cracks and serious corrosion could be observed where the layer scaled off, and the whole surface kept smooth and so no whole grain fell off though the size of grains was different (Fig. 10(b)). Specimen G still kept the drawn residual carbonaceous film on the outer surface and no alloy substrate could be observed (Fig. 10(c)).

4 DISCUSSION

During the processing of Cu-Ni alloy tubes, drawing and pulling make the inner microstructure be changed and especially the outer surface of the tubes contacted with the drawing and pulling tool has stronger deformation than the inner surface. As each grain is forced differently and begins to deform not at the same time since each one has its own particular orientation, all grains must coordinate their neighbors in deformation to keep the continuity of microstructure. Dislocations augment and move during the deformation of the alloy. If deformation is small, the dislocation tangle forms for dislocation interaction within grains. With the increase of deformation, grains are composed of smaller zones (walls of cells) divided by small angle grain boundaries, which consist of three dimensional dislocation tangle web with high density of dislocations[17]. When the pulling of Cu-Ni alloys is small, the deformation near the outer surface is relatively bigger and so the number of dislocation cells within grains increases and their size becomes smaller; while the deformation near the inner surface is relatively smaller and so dislocation cells within grains are fewer and bigger. In following annealing, deformed grains are recrystallized and new grains without strain form if their inner energy is up to the driving force needed for recrystallization, e. g. specimen H. If deformation is small, e. g. specimen A, B, C, E and F, the density of dislocations is relatively low but grains are different from one another. Only grains near the outer or inner surface of the tubes are recrystallized for their big deformation,

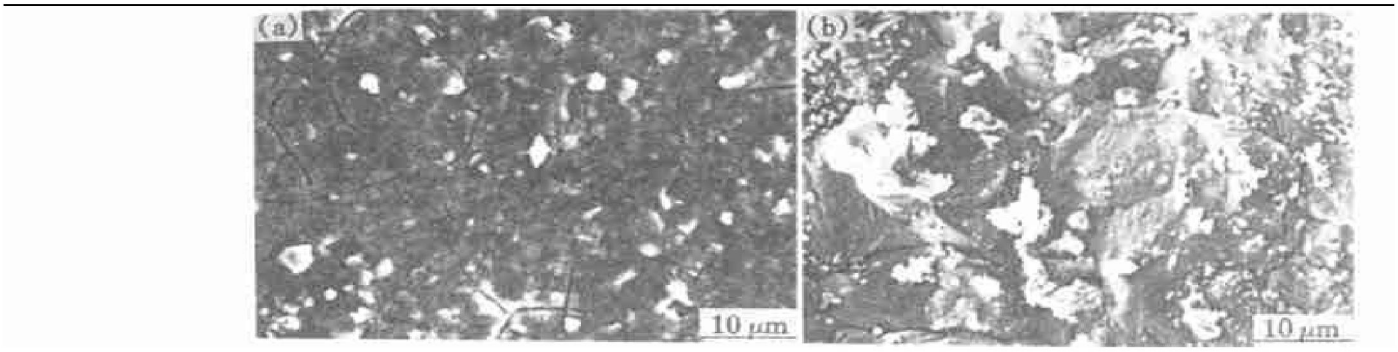

Fig. 9 Corrosion morphologies of Cu-Ni alloy tubes immersed in natural seawater for 48 months
(a) —Specimen H; (b) —Specimen A

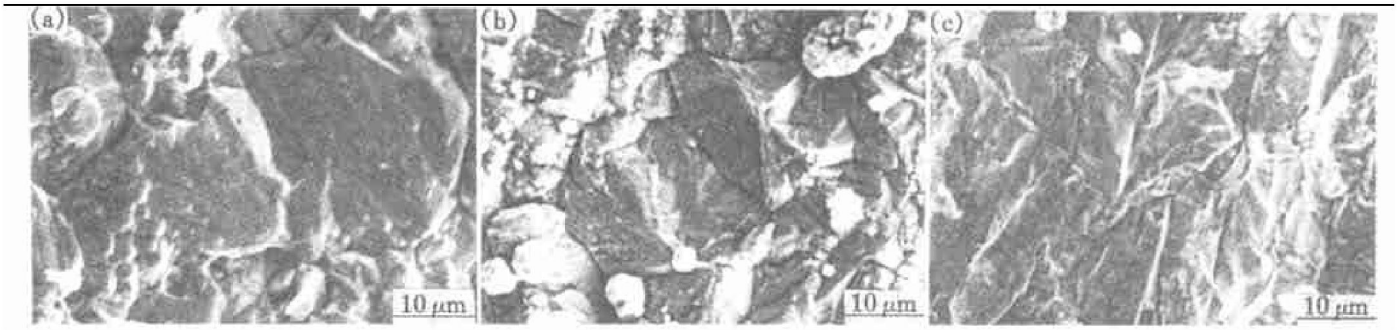

Fig. 10 Corrosion morphologies of Cu-Ni alloy tubes immersed in natural seawater for 12 months
(a) —Specimen E; (b) —Specimen F; (c) —Specimen G

whereas grains whose energy is not up to the driving force needed for recrystallization still keep in the original strain state. In fact, even different parts within one grain are not the same in deformation and it leads some grains to be partly recrystallized.

In the past research, no attention has been paid to the effect of deformation before heat treatment on the final microstructure. From the above results of Cu-Ni alloy tubes, it is known that annealing time has little effect on the microstructure at the same deformation. As deformation increases, the volume fraction of recrystallization of the tubes increases and so their microstructure becomes obviously homogeneous. Deformation has more impact on microstructure, to some extent, than heat treatment does. Thus, the proper coordination of deformation and heat treatment can distinctly improve the corrosion resistance by obtaining homogeneous solid solution at the constant chemical composition. On the contrary, the improper coordination of them results in inhomogeneous microstructure and even discontinuous precipitates on grain boundaries[18]. As to Cu-Ni allovs with incomplete recrystallization consisting of deformed and recrystallized grains, corrosion cells will be built for different corrosion potentials between deformed (high potential) and recrystallized (low potential) grains in seawater. Consequently, corrosion preferably proceeds along the boundaries between deformed and recrystallized grains since the distance of electronic transportation on boundaries between is shortest and so it leads to intergranular corrosion. On the other hand, the corrosion of deformed grains and/or along the boundaries is accelerated. The corrosion product film of Cu-Ni alloy tubes with incomplete recrystallization forms by inhomogeneous way and so is loose and porous. The original strain state including residual stress and dislocations accelerates the ionic diffusion and the occurrence of cracks of the corrosion product film, so the film easily scales off for residual stress. With the increase of the volume fraction of recrystallization, the homogeneity of microstructure increases and so grain boundaries preferring to corrosion become fewer. Besides, the decrease of residual stress and dislocation density slows the dissolution of the alloy and the uniformity and compactness of the corrosion product film increase. Therefore, the protective corrosion product film will form on the surface of recrystallized Cu-Ni alloy tubes in seawater.

5 CONCLUSIONS

1) Deformation has more impact on the final microstructure of Cu-Ni alloy tubes than the annealing time does. The alloy tubes are recrystallized if deformation is over 32%, and annealing at 550~ 600 ℃ for 1 h.

2) As the volume fraction of recrystallization increases, the homogeneity of the microstructure of Cu-

Ni alloy tubes increases and the passive zone of anodic polarization becomes wider and the corrosion rate slows down in seawater.

3) The initial surface film of Cu-Ni alloy tubes can influence the formation and protective characteristics of the corrosion product film. The residual carbonaceous film on the inner surface of the tubes during processing accelerates the dissolution of the alloy for the good electronic conductivity and the difference of potential between the carbonaceous film and the alloy substrate and results in the formation of the loose corrosion product film.

4) Immersed in natural seawater for a long period of time, e. g. 48 months, Cu-Ni alloy tubes with incomplete recrystallization corrode to be perforated and display intergranular corrosion since corrosion cells build up between deformed and recrystallized grains for their difference of corrosion potentials and electronic transportation being the shortest way along grain boundaries, while the uniform and compact corrosion product film forms on recrystallized alloy tubes for the uniformity of microstructure in seawater.

REFERENCES

[1] ZHU Xiao-long, LIN Le-yun and LEI Ting-quan. Review on corrosion behaviors of Cu-Ni alloys in seawater [J]. Corrosion Science and Protection Technology, (in Chinese), 1997, 9(1): 48~ 55.

[2] Gilbert P T. A review of recent work on corrosion behavior of copper alloys in sea water [J]. Materials Performance, 1982, 21(2): 47~ 50.

[3] Efird K D. The synergistic effect of Ni and Fe on the sea water corrosion of copper alloy [J]. Corrosion, 1977, 33: 347~ 351.

[4] Drolenga L J P, IJsseling F P and Kolster B H. The influence of alloy composition and microstructure on the corrosion behaviour of Cu-Ni alloys in seawater [J]. Werkstoffe und Korrosion, 1983, 34: 167~ 172.

[5] Beccaria A M, et al. Influence of heat treatment on pitting sensitivity of Cu-Ni 70/30 alloy in sea water of different temperature [J]. Werkstoffe und Korrosion, 1994, 45: 562~ 565.

[6] Richter F and Pepperhoff W. Mossbauer-spektrometrie an magnetisch geordneten ausscheidungen im system Cu-Ni-Fe [J]. Werkstoffe und Korrosion, 1983, 34: 161~ 166.

[7] ZHU Xiao-long and LEI Ting-quan. Influence of deformation and heat treatment on seawater corrosion of 70Cu-30Ni alloy [J]. J Mater Sci Technol, 1998, 14(1): 57~ 61.

[8] ZHU Xiao-long. Influence of deformation and heat treatment on marine corrosion of 70Cu-30Ni alloy [D]. PhD Dissertation. Harbin: Harbin Institute of Technology, 1996: 19.

[9] Marsden D D. Early failure of cupro-nickel heat exchanger tubes—a case history [J]. Materials Performance, 1978, 17(8): 9~ 12.

[10] Nagata K, Atsumi T and Yonemitsu M. Effect of initial surface on the corrosion resistance of CN 108 alloy tube in sea water [J]. Sumitomo Light Metal Technical Reports, 1992. 33(4): 20~ 24.

[11] IJsseling F P, Drolenga L P J and Kolster B H. Influence of temperature on corrosion product film formation on CuNi10Fe in the low temperature range: Corrosion rate as a function of temperature in well aerated sea water [J]. British Corrosion Journal, 1982, 17(4): 162~ 167.

[12] IJsseling F P, Krougman J M and Drolenga L J P. The corrosion behaviour of the system CuNi10Fe/seawater: the protective layer of corrosion products [A]. In: 5th Internal Congress on Marine Corrosion and Fouling, (Corrosion) [C]. Barcelona: May 1980: 146~ 168.

[13] Bjourndahl W D and Nobe K. Copper corrosion in chloride media: Effect of oxygen [J]. Corrosion, 1984, 40(1): 82~ 86.

[14] Moreau A, et al. E tude du me D' oxyDo reduction du cuivre dans les solution chlorurees acides II Systemes Cu-CuCl-$CuCl_2^-$ et Cu-$Cu_2(OH)_3Cl$-$CuCl^+$-Cu_2^{2+} [J]. Electrochimica Acta, 1981, 26: 1609~ 1614.

[15] Dhar H P, et al. Corrosion behavior of 70Cu-30Ni alloy in 0.5 M NaCl and in synthetic seawater [J]. Corrosion, 1985, 41(4): 193~ 198.

[16] Deslouis C and Tribollet B. Electrochemical behaviour of copper in neutral aerated chloride solution. I. Steady-state investigation [J]. Journal of Applied Electrochemistry, 1988, 18: 374~ 378.

[17] Borxin P I. Physical Basis of Plastic Deformation [M]. Huan Keqing, et al transl. Beijing: Metallurgical Industry Press, 1989: 216.

[18] ZHU Xiao-long. Influence of the microstructure of Cu-Ni alloy on its corrosion resistance [J]. Transaction of Nonferrous Metals Society of China, 1992, 2(4): 51~ 55.

(Edited by YUAN Sai-qian)